Characterization of Functionalized Plasmonic Substrates for SERS Applications

Author: Maria Serra González
*Facultat de Física, Universitat de Barcelona, Diagonal 645, 08028 Barcelona, Spain.**

Advisor: Arantxa Fraile Rodríguez

Abstract: The effect of topography in the Raman signal from solutions of 4-mercaptopyridine molecules is determined when deposited with different concentrations on two different Au substrates with plasmonic properties: continuous thin films and ordered lattice of nanoelements. The topography is characterized through Atomic Force Microscopy imaging. The results show how the nanostructured substrate affects the topography presenting similar configuration to more diluted solutions.

I. INTRODUCTION

The first observation of enhanced Raman spectra was reported in 1974 [1]. But it was not until 1977, that Van Duyne and Albrecht discovered surface-enhanced Raman scattering (SERS) [2, 3] as a phenomenon with outstanding enhancement of Raman signals from molecules that are near metallic nanostructures. It is a sensitive, vibrational spectroscopic technique capable of giving rich, molecularly specific information.

The enhancement factor is strongly dependent on the substrate and it is based on the combination of two mechanisms. The most relevant is the electromagnetic field enhancement, associated with localized surface plasmons of metallic nanostructures. It enhances the Raman signal by a factor of $10^{10} - 10^{11}$ [4], depending on the surface structure and metallic material. The second mechanism is the chemical enhancement, where the charge is transferred between the adsorbed molecule and the metal. It increases the Raman intensity up to 10^3 as theoretically calculated by L. Jensen et al. [5].

These last decades, interest in SERS has exponentially grown in various research fields. Although, few studies have been carried out where the morphology of the studied samples and Raman spectra were combined. It has been done with Ag substrates [7], where Ag colloidal nanoparticles were deposited on roughened Ag substrates enhancing their Raman signal.

In our work, we have studied the detection limit of Raman spectroscopy in functionalized plasmonic substrates, by changing the concentration and the volume of the analytes deposited on top. Finally, AFM imaging was done for every Raman measure in order to characterize the sample's topography. Continuous and nanostructured gold (Au) substrates were considered in order to evaluate SERS effects. In particular, solutions of literature's standard 4-mercaptopyridine (4-Mpy) molecules were prepared and used to functionalize the different Au substrates mentioned.

*Electronic address: maria.serra.20297@gmail.com

II. SAMPLE PREPARATION

A. Substrates

Two different Au substrates were used in this study produced by A.Conde-Rubio [8, 9]. The first type of substrate used is what it will be called continuous Au. It consists on a $100nm$-thick homogeneous Au layer deposited upon a Si substrate by Electron Beam Evaporation (EBE) using a $5nm$-thick Ti layer to enhance the adhesion.

The second type is a nanoelement structure consisting on a hexagonal lattice of asterisk-shaped holes. The sample fabricated has twenty-four areas distributed in four rows (labeled with numbers) and six columns (labeled with letters), on a continuous Au base surface, as seen in Fig. 1. Each row number indicates a different dose factor (DF) used during the Electron Beam Lithography (EBL) production. In this study, only A4 and D3 areas were used.

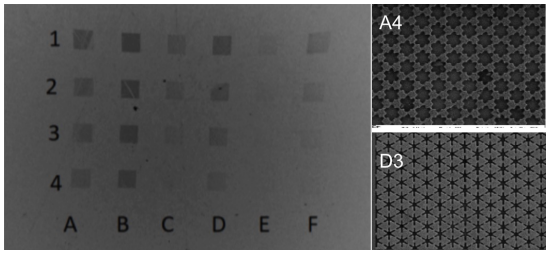

Figure 1: Left, SEM micrography of the Au nanostructured sample. Right, magnification of the areas used in this study, A4 and D3.

B. Functionalization

All samples were functionalized through the same process, either for the continuous and the nanostructured Au, at the laboratories of the Magnetic Nanomaterials Group from the UB.

The sample needs to be cleaned with deionized water, and N_2 gas is used to blow the residual water droplets.

The cleaning procedure reduces background noise on the SERS measurement. Eliminating leftover molecules on the surface creates a better environment for the 4-Mpy molecules to bind with the surface.

Using different micro pipettes, three different droplets were pipetted and deposited into different areas of the continuous Au and one droplet into the nanostructured Au. After each deposition, the samples were dried on the oven at 80^oC for 5 min. The different depositions that were employed are listed next.
Continuous Au:

- droplet 1: $2\mu L$ from $3 \cdot 10^{-3}M$ solution
- droplet 2: $0.5\mu L$ from $10^{-6}M$ solution
- droplet 3: $2\mu L$ from $10^{-6}M$ solution

Nanostructured Au:

- droplet 4: 0.5μ L from $10^{-6}M$ solution

III. CHARACTERIZATION

A. Raman

The structural Raman fingerprint of 4-Mpy was obtained in a Jobin-Yvon LabRam HR 800 dispersive spectrometer coupled to an Olympus BXFM optical microscope with a x100 objective from the Centres-Científico-Tecnològics of the Universitat of Barcelona (CCiTUB).

In Raman, the change of frequency between incident light, from the spectrometer's laser, $\lambda = 785nm$, and detected light, from desexcitations of the molecule's electrons, is measured and it is called Raman Shift. Our measurement procedure was as follows:

After finding the area of interest with the Raman's optical microscope, the laser is activated and focused and the acquisition is started. The parameters chosen were Time of acquisition = $30s$ and Laser intensity = 100% in all cases.

The focusing points studied were ranged from the interior to the exterior of the droplet passing through the edge, where most of the molecules were deposited. Considering a circular distribution, the differences in the molecules' deposition were relevant in radial changes and not in angular changes, so it was not very significant if the studied points were not exactly in the same angular section.

In the case of the nanostructured Au substrates, the laser is focused on the A4 area where the molecules were deposited, and then it is changed to the D3 area where no molecules are deposited at all.

Afterwards, the Raman signals were analyzed using Origin software subtracting a baseline and finding the main peaks. Then the peaks were assigned to the 4-Mpy vibrational peaks on the literature [10].

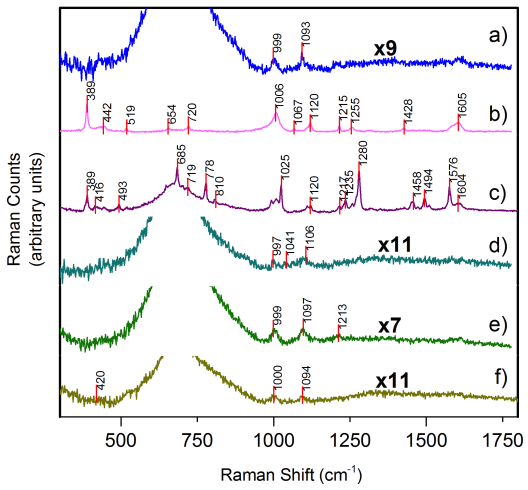

Figure 2: Raman spectra as moving radially on the droplet: exterior a), edge's limit b), edge's center c), interior d),e) and center of the droplet f). Raman counts in arbitrary units in order to show how much more intense are peaks on the edge of the droplet than in the rest of the areas.

B. AFM

To characterize the sample's topography, an Atomic Force Microscope in the CCiTUB was used. AFM is a high-resolution scanning probe microscope with spatial resolution on the order of nanometers. It allows to make a visual inspection of the deposited molecules and obtain parameters such us roughness, height of the atomic steps or number of layers in the sample. The AFM used works in tapping mode. First, a video camera was used to position the selected sample area for the AFM scan. Next, the tip was focused and engaged, in order to start the AFM scanning. Parameters such as Scan Size, Pixels per Line and Scan Frequency were modified depending on the image being taken. The AFM images were not recorded exactly at the same spots as the Raman spectra but in equivalent positions.
A flatten filter (2n and 3rd order) was applied to all images to correct tilts and bows of the background.

IV. ANALYSIS AND RESULTS

A. Continuous Au

Droplet 1 (2μL and $3{\cdot}10^{-3}$M)

For the concentrated droplet, six different Raman spectra were taken from the interior to the exterior of the droplet, shown in Fig.2. In Figs.2 b) an c) 4-Mpy characteristic peaks appear. This shows that in a droplet type deposition, molecules will deposit mainly on the circular edge of the droplet.

Also, between the spectra in Fig.2 b), edge's exterior limit, and Fig.2 c), edge's center, exist changes in the

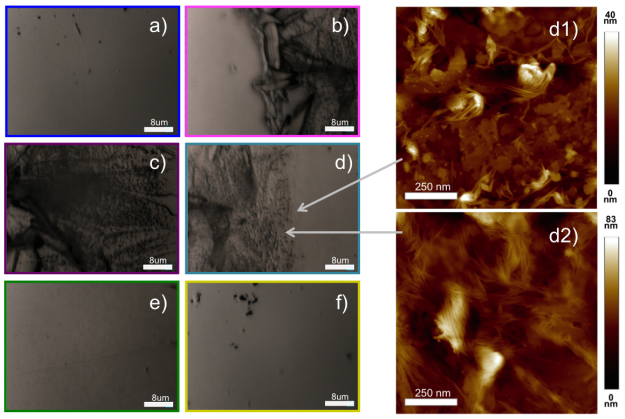

Figure 3: Raman's x100 magnification microscope (left) and AFM images (right). The Raman images correspond exactly to the spectra from Fig.2. The arrows pointing to area d) show approximately the only two spots where AFM had good results.

peaks and in intensity, confirming that differences in the deposition are found in a radial, rather than in an angular, distribution.
The Appendix shows a detailed assignation of the Fig.2 c) peaks indicating the corresponding vibrational states.

It is worth stressing that 4-Mpy peaks that appear in Figs.2 a), e) and f) are probably associated with a poor washing of the sample. This sample had been formerly dip coated in 4-Mpy solutions. Although having been cleaned several times, a weak signal around $\sim 1005cm^{-1}$ and $\sim 1099cm^{-1}$ peaks appear (corresponding to *Ring breathing* and *Trigonal ring breathing with C-S* vibrational states), showing that residues are still present outside the droplets' edge. These peaks will appear in the following spectra as well.

It is also relevant the disappearance of the characteristic Au wide peak in the spectrum shown in Fig.2 b). It shows that the molecule's layer thickness on the edge limit is bigger than Raman's laser penetration depth, which is $< 10\mu m$. This gives us an estimation of the thickness of the layer.
To know the exact thickness, the layer's step height from AFM images should be calculated. Unfortunately, it was not possible due to technical AFM issues. The AFM's tip is very close to the surface and operates in tapping mode. If it encounters large topographic differences, large instabilities appear while scanning and image cannot be recorded. Only two images were able to be acquired in the inner limit of the edge, Figs.3 d1) and d2). In Raman's optical microscopy image in Fig.3 d), the approximate points where these images were taken are pointed with arrows.

In Fig.3 d2) stands out the fibrilar structure of the 4-Mpy. In Fig.3 d1) a few fiber structures are still seen but structures in flake shape appear. This last area is equivalent to Fig.2 d) Raman spectrum. Although 4-Mpy peaks are not seen in this spectrum, in the AFM image, molecules' deposition is observed. The change in the topography, as we get further radially from the limit's droplet edge, shows the heterogeneity in the molecules' deposition on the substrate. This topic will be further discussed later in another context.

Droplet 2 (0.5μL and 10^{-6}M)

The second droplet deposition was made with the second solution following the same procedure. The three analyzed spectra are shown on Fig.4. The three order of magnitude reduction of the solution prevents the apparition of the majority of 4-Mpy peaks seen in Fig.2 b) and c). As it was pointed out in the previous section, the peaks $\sim 1005cm^{-1}$ and $\sim 1099cm^{-1}$ appear due to a poor washing of the substrate. However, in spectrum Fig.4b) a weak increase in intensity from these above mentioned peaks is appreciated. It can be concluded that the deposition of a droplet from a $10^{-6}M$ 4-Mpy solution is near the Raman's detection limit in this substrate, but still perceptible.

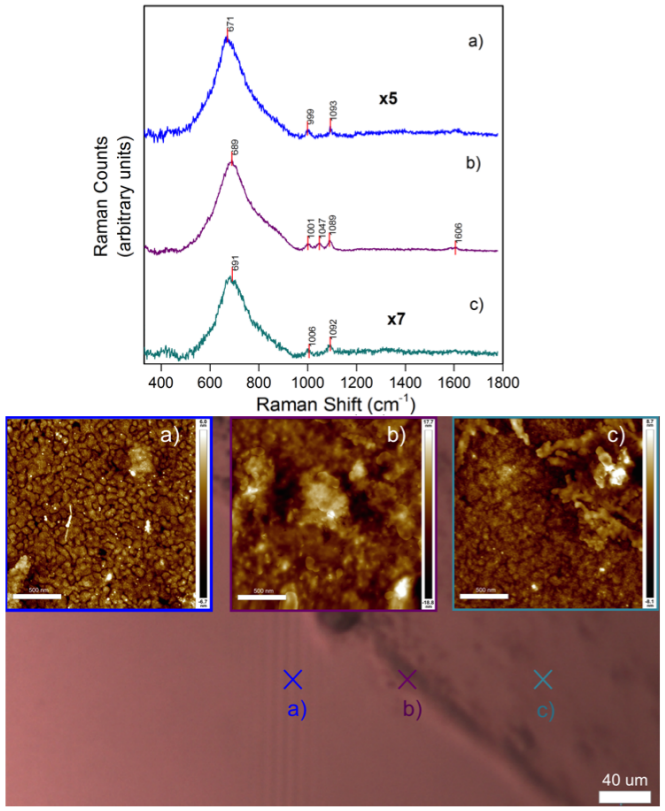

Figure 4: On top, Raman spectra from the exterior a), the limit's edge b), and the center of the edge c) of the droplet. In arbitrary units, it shows the augment needed to have a similar peak size as the b) spectrum, measured on the area where most molecules are deposited. On the bottom background, Raman microscope's x100 image of a droplet edge's section. The a), b) and c) cross marks correspond approximately to the AFM images on the top (with Scan Size = $2\mu m$).

The topography of the deposition using AFM is dis-

played at the bottom of Fig.4.

The three images are taken by AFM and correspond to the three Raman spectra. They clearly show a different topography from the previous concentrated droplet. A mix between terrace and flake structures can be seen in the image from the edge's limit. It is very clear again, the change in topography between the limit, Fig.4 b), and the center of the edge, Fig.4 c).

Droplet 3 (2μL and 10^{-6}M)

The third's droplet deposition was made with a higher volume from the $10^{-6}M$ solution following the same procedure. Fig.5 shows the three analyzed spectra. The low concentration prevents the apparition of the majority of 4-Mpy's peaks again. It is clear the similarity with Fig.4 meaning that the solution's concentration is the key factor rather than the droplet's volume. The two $\sim 1005cm^{-1}$ and $\sim 1099cm^{-1}$ peaks appear again in the three spectra but again sightly increased in Fig.5 b), as it was expected. It can be concluded from the current and the previous sections that the deposition of a droplet from a $10^{-6}M$ 4-Mpy solution is near the Raman's detection limit although still visible.

However, in the AFM images at the bottom of Fig.5, the differences in topography, when compared to the image in Fig.4, are remarkable. Cubic-like crystallization appears for the first time in the edge area, Fig.5 b), where most of the molecules are deposited, according to the Raman spectra in Fig.5. Moving to the interior of the droplet, the molecules tend to form more elongated structures, Fig.5 c). The deviation in morphology as moving radially from the limits edge to the center of the droplet, is thoroughly discussed by Marín et al. in [11]. This phenomenon is explained thanks to a transition of the order-to-disorder phase due to a singularity in the drying velocity inside the evaporating droplet at the end of its life. When the deposition speed is low, particles have time to arrange by Brownian motion, while at the end, high-speed particles are wedged into a disordered phase. This argumentation is extensible to the two prior sections, as well as the following one.

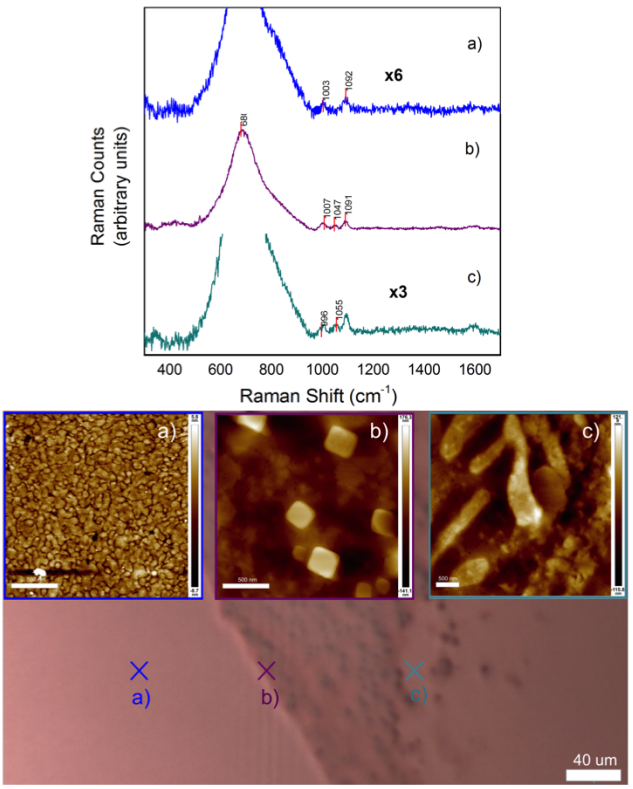

Figure 5: On top, Raman spectra from the exterior a), the limit's edge b), and the center of the edge c) of the droplet. In arbitrary units, it shows the augment needed to have a similar peak size as the b) spectrum, from an area without molecules deposited. The Au peak is cropped to show the 4-Mpy peaks clearer. On the bottom background, Raman microscope's x100 image of a droplet edge's section. The a), b) and c) cross marks correspond approximately to the AFM images on the top (Scan Size $2\mu m$ for a), b) and $4\mu m$ for c)).

B. Nanostructured Au

Droplet 4 (0.5μL and 10^{-6}M)

This time, the surface with an array of asterisk shaped nanostructures, enhances Raman signal as explained earlier. The spectra from the area with the 4-Mpy droplet, A4, and the area without it, D3, are shown in Fig.6 a) and Fig.6 b), respectively. In Fig.6 b) 4-Mpy peaks should not be seen, however, they appear associated again with a poor washing of the sample. In Fig.6 c) a spectrum of the same area A4 from [12] data, where no molecules were deposited is shown. It gives a qualitative idea of how the Au spectral shape should be for the clean A4 area.

In conclusion, the difference in Raman counts from Figs.6 a) to b) is a factor of 4, but if the sample were completely clean, the change in the peaks would have been much more significant in position and intensity. Also, the spectra are very different from Fig.4 in which the droplet's conditions were the same, meaning that changing the substrate to a nanostructure array enhances Raman signal as expected from a SERS.

Regarding the topography of the deposition, displayed in bottom Fig.6 b) and c), fibrilar structure appears again in opposition to the flake-shaped topography observed in Fig.4. It is more similar to the first concentrated droplet shown in Fig.3. It indicates that not only the Raman signal changes with a nanostructured substrate but the molecule's deposition morphology does as well.
Furthermore, in bottom image Fig.6 c) it is visible the shadow of the asterisk shape from the substrate (highlighted in dashed lines), meaning that the molecule layer thickness is thinner than in Fig.6 b).

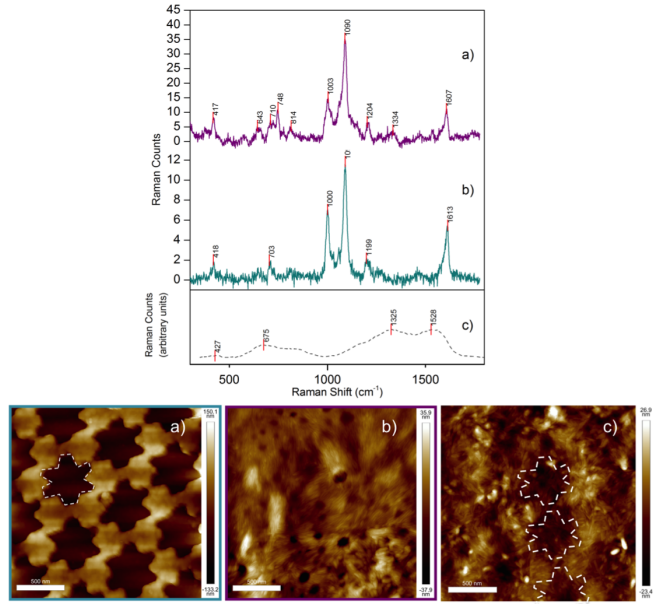

Figure 6: On top, Raman spectra from nanostructured areas with (A4) a); and without (D3) b), droplet deposition. In c), an A4 clean spectrum from [12] data to show the qualitative spectral shape (with different acquisition parameters) is displayed. On the bottom, AFM images from area A4. a), exterior (without molecules); b), edge's limit; and c), center of the edge of the droplet. In a) and c) a silhouette of the nanostructured pattern was overlapped in dashed lines.

V. CONCLUSIONS

By using Raman spectroscopy we have tracked the presence of 4-Mpy molecules with different concentration on different areas of both continuous and nanostructured Au substrates.

Combining the Raman spectra with the Atomic Force Microscopy images of similar areas, we were able to correlate the Raman results with the sample's topography in each one of them. We have seen that deposition's topography varies with concentration and volume deposited, going from fibrilar structure for the concentrated droplet, to flake-shaped layers or cubic crystallization on the diluted ones. We could see how the nanostructured substrate affects the topography showing a fibrilar configuration despite being a much more diluted solution.

It has been remarkable the change in the molecules arrangement as we moved from the limit's edge of the droplet to its center, radially, likely due to a singularity in the drying velocity of the droplet [11]. It is an extremely important aspect of the study since the deposition's topography indicates in which area measures have to be taken in diluted analytes analysis.

In further studies, different types of deposition and drying methods could be followed in order to minimize the deposition gradient and have a more homogeneous sample.

VI. ACKNOWLEDGMENTS

All my gratitude to my advisor Prof. Arantxa Fraile for her guidance, support and dedication. Many thanks to Ph.D Mariona Escoda for all her assistance, reliability and knowledge shared. Also, thanks to Aranzazu Vila, Tariq Jawhari and Isaac Godoy, for their assistance in the CCiTUB labs. Finally, thanks to my family and friends for their care and support.

[1] Fleischmann, M.; Hendra, P.J.; McQuillan, A., "Raman Spectra of Pyridine Adsorbed at a Silver Electrode", Chem. Pyhs. Lett **26**, 163-166, 1974.

[2] Jeanmaire, D.L.; van Duyne, R.P., "Surface Raman Spectroelectrochemistry: Part I. Heterocyclic, Aromatic, and Aliphatic Amines Adsorbed on the Anodized Silver Electrode". J. Electroanal. Chem. Interfacial Electrochem. , **84**, 1–20, 1977.

[3] Albrecht, M.G.; Creighton, J.A. "Anomalously Intense Raman Spectra of Pyridine at a Silver Electrode", J. Am. Chem. Soc. **99**, 5215–5217, 1977.

[4] Camden, J.P.; Dieringer, J.A.; Wang, Y.; Masiello, D.J.; Marks, L.D.; et al., "Probing the Structure of Single-Molecule Surface-Enhanced Raman Scattering Hot Spots", J. Am. Chem. Soc. **130**, 12616–12617, 2008.

[5] Jensen, L.; Aikens, C.M.; Schatz, G.C., "Electronic Structure Methods for Studying Surface-Enhanced Raman Scattering", Chem. Soc. Rev. **37**, 1061-1073, 2008.

[6] Morton, S.M.; Jensen, L., "Understanding the MoleculeSurface Chemical Coupling in SERS", J. Am. Chem. Soc. **131**, 4090–4098, 2009.

[7] Muniz-Miranda, M; Pergolese, B; Bigotto, A; Giusti, A,"Stable and Efficient Silver Substrates for SERS Spectroscopy", J. Colloid and Interface Science **314** (2), 540-544, 2007.

[8] Conde-Rubio, A; Rodríguez, A.F.; Borrisé, X.; Perez-Murano, F.; Batlle, X.; et al, "Geometric Frustration in a Hexagonal Lattice of Plasmonic Nanoelements", Optics express **26** (16), 20211-20224, 2018.

[9] Conde-Rubio, A., "Simulations, Nanofabrication and Optical Characterization of Plasmonic Nanostructures" Doctoral dissertation, 2018. Retrieved from `https://magneticnanomaterialsub.files.wordpress.com/2018/11/tesisacr.pdf`

[10] Zhang, L.; Bai, Y.; Shang, Z.; Zhang, Y.; Mo, Y., "Experimental and Theoretical Studies of Raman Spectroscopy on 4-mercaptopyridine Aqueous Solution and 4-mercaptopyridine/Ag Complex System". J. Raman Spectrosc. **38**, 1106-1111 2007.

[11] Marín, A. G. et al, "Order-to-Disorder Transition in Ring-Shaped Colloidal Stains". Phys. Rev.Lett. **107**, 2011.

[12] Roca, I. "Functionalized plasmonic lattices for biomolecule detection". TFG UB 2019.

Appendix

Raman Shift Peaks (cm^-1)	Wavenumber (cm^-1)	Assignation
389	389 w	———
493	489 vw	C-C-C stretch
718	712 m	out-of-plane C-H def
778	777 vw	In-plane C-H def
810	809 vw	———
1025	1028 w	In-plane C-H def
1120	1131 w	C-H def
1217	1217 s	In-plane C-H def
1280	1279 vw	In-plane C-H def
1576	1581 vs	Ring stretch with N
1604	1612 s	Ring stretch with N

TABLE I: Raman Shift peaks found in Fig.2 c) spectrum, wavenumber from 4-Mpy characteristic peaks found in literature, [10], with the notation *w* for weak peaks, *vw* for very weak, *m* for medium, *s* for strong and *vs* for very strong, and vibrational mode assigantion.